Published OnlineFirst July 14, 2010; DOI: 10.1158/0008-5472.CAN-10-0184

Cancer Research

Circadian Rhythm of Transferrin Receptor 1 Gene Expression Controlled by c-Myc in Colon Cancer–Bearing Mice

Fumiyasu Okazaki[1], Naoya Matsunaga[1], Hiroyuki Okazaki[1], Naoki Utoguchi[2], Ryo Suzuki[2], Kazuo Maruyama[2], Satoru Koyanagi[1], and Shigehiro Ohdo[1]

Abstract

The abundance of cell surface levels of transferrin receptor 1 (TfR1), which regulates the uptake of iron-bound transferring, correlates with the rate of cell proliferation. Because TfR1 expression is higher in cancer cells than in normal cells, it offers a target for cancer therapy. In this study, we found that the expression of TfR1 in mouse colon cancer cells was affected by the circadian organization of the molecular clock. The core circadian oscillator is composed of an autoregulatory transcription-translation feedback loop, in which CLOCK and BMAL1 are positive regulators and the *Period* (*Per*), *Cryptochrome* (*Cry*), and *Dec* genes act as negative regulators. TfR1 in colon cancer–bearing mice exhibited a 24-hour rhythm in mRNA and protein levels. Luciferase reporter analysis and chromatin immunoprecipitation experiments suggested that the clock-controlled gene *c-MYC* rhythmically activated the transcription of the *TfR1* gene. Platinum incorporation into tumor DNA and the antitumor efficacy of transferrin-conjugated liposome-delivered oxaliplatin could be enhanced by drug administration at times when TfR1 expression increased. Our findings suggest that the 24-hour rhythm of TfR1 expression may form an important aspect of strategies for TfR1-targeted cancer therapy. *Cancer Res; 70(15); 6238–46. ©2010 AACR.*

Introduction

In mammals, the master pacemaker controlling the circadian rhythm is located in the suprachiasmatic nuclei of the hypothalamus (1). Regulation of circadian physiology relies on the interplay of interconnected transcription-translation feedback loops. The BMAL1/CLOCK complex activates clock-controlled genes, including *Per, Cry*, and *Dec*, the products of which act as repressors by interacting with BMAL1/CLOCK (2–5). This mechanism also regulates the 24-hour rhythm in output physiology through the periodic activation/repression of clock-controlled output genes in healthy peripheral tissue and tumor tissue (6, 7).

Transferrin receptor 1 (TfR1) is involved in the uptake of iron into cells through the binding and internalization of transferrin, and its regulation by intracellular iron levels has assisted in the elucidation of many important aspects of cellular iron homeostasis (8, 9). Iron is important for metabolism, respiration, and DNA synthesis. Thus, TfR1 is expressed not only in normal healthy cells but also in malignant tumor cells (8, 10). Recently, another TfR-like molecule named TfR2 has been recognized and investigated (11, 12), but the exact function of TfR2 remains unclear (8). It has been reported that the expression of TfR1 in mammary epithelial cells exhibits a significant 24-hour rhythm (13). Such rhythmic variation in TfR1 expression seems to affect its iron uptake function resulting in time-dependent changes in the internalization of iron-loaded Tf. However, it is not clear if the expression of TfR1 in colon cancer cells shows a significant 24-hour rhythm.

Many of the pharmacologic properties of conventional drugs can be improved through the use of an optimized drug delivery system (DDS), which includes particular carriers composed primarily of lipids and/or polymers (14). The high expression of TfR1 in tumor can potentially be used to deliver cytotoxic agents into malignant cells, including chemotherapeutic drugs, cytotoxic proteins (8), and Tf-coupled polyethylene glycol (Tf-PEG) liposomes were designed as intracellular targeting carriers for drugs by systemic administration. In fact, Tf-PEG liposomes encapsulating a platinum (Pt)-based anticancer drug, oxaliplatin, can increase its accumulation in tumor masses (15, 16). On the other hand, daily rhythmic variations in biological functions are thought to affect the efficacy and/or toxicity of drugs: a large number of drugs cannot be expected to have the same potency at different administration times (7, 17). However, it is unclear what influence the rhythmic expression of TfR1 has on the pharmacokinetics/pharmacodynamics of transferrin targeting liposomes.

Authors' Affiliations: [1]Department of Pharmaceutics, Graduate School of Pharmaceutical Sciences, Kyushu University, Fukuoka, Japan and [2]Department of Pharmaceutics, Teikyo University, Sagamiko, Sagamihara, Japan

Note: Supplementary data for this article are available at Cancer Research Online (http://cancerres.aacrjournals.org/).

F. Okazaki, N. Matsunaga, and S. Ohdo contributed equally to this work.

Corresponding Author: Shigehiro Ohdo, Department of Pharmaceutics, Graduate School of Pharmaceutical Sciences, Kyushu University, Fukuoka, 812-8582, Japan. Phone: 81-92-642-6610; Fax: 81-92-642-6614; E-mail: ohdo@phar.kyushu-u.ac.jp.

doi: 10.1158/0008-5472.CAN-10-0184

Published OnlineFirst July 14, 2010; DOI: 10.1158/0008-5472.CAN-10-0184

In this study, we found that the circadian expression of *c-Myc*, which is controlled by the circadian clock, affects *TfR1* gene transcription in colon cancer cells. The levels of *TfR1* mRNA and protein exhibited a 24-hour oscillation in tumor cells implanted in mice. Thus, to evaluate the rhythmic function of TfR1 and the utility for TfR1-targeting cancer therapy, we investigated how the rhythmic variation in TfR1 production influenced the pharmacologic efficacy of TfR1-targeting liposomal DDS.

Materials and Methods

Animals and cells

Seven-week-old male BALB/c mice (Charles River Japan) were housed with lights on from 7:00 a.m. to 7:00 p.m. at a room temperature of 24 ± 1°C and a humidity of 60 ± 10% with food and water *ad libitum*. Colon 26 cells (Cell Resource Center for Biomedical Research, Tohoku University) were maintained in RPMI 1640 supplemented 10% fetal bovine serum (FBS) at 37°C in a humidified 5% CO_2 atmosphere. A 25-μL volume with 2×10^7 viable tumor cells was inoculated into the right hind footpad of each mouse. The tumor volume was estimated according to a formula that has been described previously (7). Tissue slices of the removed tumor masses were made, and the tumor tissue was confirmed histopathologically.

Experimental design

To assess the temporal expression profile of TfR1 in tumor cells, tumor masses were removed from individual tumor-bearing mice at six different time points (9:00 a.m., 1:00 p.m., 5:00 p.m., 9:00 p.m., 1:00 a.m., and 5:00 a.m.) 7 days after the implantation of tumor cells. The levels of *TfR1* protein and mRNA were measured by Western blotting analysis and quantitative reverse transcription-PCR (RT-PCR), respectively. To investigate how the rhythmic variation in *TfR1* expression occurs in tumor cells, the influence of CLOCK/BMAL1 and c-MYC on the transcriptional activity of the *TfR1* gene was assessed using luciferase reporter constructs containing wild-type E-box or mutated E-box of the mouse *TfR1* promoter, which was based on previous reports. To elucidate the role of c-MYC in the control of the rhythmic expression of *TfR1*, endogenous c-MYC in Colon 26 cells was downregulated by small interfering RNA (siRNA). The c-MYC–downregulated cells were treated with 50% FBS for 2 hours to synchronize their circadian clock, and the mRNA levels of *TfR1* were assessed at 44, 48, 52, 56, 60, 64, and 68 hours after 50% serum treatment. In the same manner as described above, the protein levels of c-MYC and CLOCK were assessed by Western blotting analysis. To explore the temporal binding of endogenous c-MYC and CLOCK to the E-box in the mouse *TfR1* gene, chromatin immunoprecipitation analysis was performed in individual tumor masses at 9:00 a.m. and 9:00 p.m. To investigate the function of the 24-hour oscillation of TfR1 expression, time-dependent changes in Pt internalization into tumor cells were assessed using Tf-coupled liposomes encapsulating oxaliplatin (Tf-NGPE L-OHP). The cultured Colon 26 cells were treated with 50% FBS as described above and then harvested for RNA extraction at 0, 6, 12, 18, and 24 hours after 50% FBS treatment. Nontreated Colon 26 cells harvested at the same time points were used as the control. At 6 or 18 hours after serum treatment, cells were exposed to Tf-NGPE L-OHP (L-OHP, 0.4 mg/mL) for 3 hours. The Pt content in the DNA was measured using an inductively coupled plasma mass spectrometer (ICP-MS). To explore the dosing time–dependent difference in the internalization of Pt into tumor cells *in vivo*, tumor-bearing mice were injected with a single dose of Tf-NGPE L-OHP at 9:00 a.m. or 9:00 p.m. Plasma and tumor DNA samples were collected only once from individual mice at 1, 3, and 6 hours after injection. The plasma concentration of Pt and its content in tumor DNA were measured as described above. Then, tumor volumes were measured throughout the duration of the experiment.

RT-PCR analysis

Total RNA was extracted using RNAiso (TaKaRa). The cDNAs of mouse *TfR1* (NM011638), *TfR2* (NM015799), *c-Myc* (NM010849), and β-*actin* (NM007393) were synthesized using PrimeScript Reverse Transcriptase (TaKaRa), and the synthesized cDNAs were amplified using GoTaq Green Master Mix (Promega). The PCR products were run on 2% agarose gels. After staining with ethidium bromide, the gel was photographed using Polaroid-type film. The density of each band was analyzed using NIH image software on a Macintosh computer. To evaluate the quantitative reliability of RT-PCR, kinetic analysis of the amplified products was performed to ensure that signals were derived only from the exponential phase of amplification, as previously described (7, 17). We evaluated the validity of our semiquantitative PCR methods using real-time PCR. cDNA was prepared by reverse transcription of total RNA. Real-time PCR analysis was performed on diluted cDNA samples with SYBR Premix Ex Taq Perfect Real-Time (TaKaRa) using a 7500 Real-time PCR system (Applied Biosystems). In addition, as confirmation of RNA extraction from each tumor cell sample, the expression level of *Vegf* mRNA was measured (Supplementary Data S1).

Western blotting analysis

Nuclear or cytoplasmic proteins in tumor masses were extracted using NE-PER Nuclear and Cytoplasmic Extraction Reagents (Pierce Biotechnology). The protein concentrations were determined using a BCA Protein Assay kit (Pierce Biotechnology). The lysate samples were separated on 6% or 10% SDS-polyacrylamide gels and transferred to polyvinylidene difluoride membranes. The membranes were reacted with antibodies against TfR1 (Zymed Laboratories), c-MYC, CLOCK, β-actin (Santa Cruz Biotechnology), or RNA pol II (Abcam). The immunocomplexes were further reacted with horseradish peroxidase–conjugated secondary antibodies and visualized using Super Signal Chemiluminescent Substrate (Pierce Biotechnology). The membranes were photographed using Polaroid-type film, and the density of each band was analyzed using NIH image software on a Macintosh computer.

Published OnlineFirst July 14, 2010; DOI: 10.1158/0008-5472.CAN-10-0184

Construction of reporter and expression vectors

The 5′ flanking region of mouse *TfR1* (from bp +16 to +436; +1 indicates the transcription start site) gene was amplified using Elongase Enzyme mix (Invitrogen) using DNA extracted from Colon 26 cells. PCR was performed using the forward primer 5′-AGTTGAGCTC(*Sac*I)GGCTTGGTGCAGCTCAGTTAGTAG-3′ and reverse primer 5′-ATGAGATATC(*Eco*RV)TAAATGTCCGTTGACACTAGTAACC-3′. The PCR products were purified and ligated into a pGL4 Basic vector (*TfR*1-Luc). The sequence of the CACGTG E-box (bp +290 to +295) on *TfR*1-Luc was mutated using a QuikChange site-directed mutagenesis kit (Stratagene). Expression vectors for mouse CLOCK, BMAL1, and c-Myc were constructed using cDNAs obtained from RT-PCR derived from mouse liver RNA. All coding regions were ligated into the pcDNA3.1 (+) vector (Invitrogen), as previously described (7). Protein expression levels from each expression vector in Colon 26 were assessed by Western blotting analysis (Supplementary Data S2).

Luciferase reporter assay

Colon 26 cells were seeded at 3×10^5 cells per well in six-well culture plates (BD Biosciences). After an 18-hour culture, the cells were transfected with 100 ng per well of reporter vector and 2 μg per well (total) of expression vector using Lipofectamine LTX reagent (Invitrogen). A 0.5-ng-per-well sample of phRL-TK vector (Promega) was also cotransfected as an internal control reporter. The total amount of DNA per well was adjusted by adding pcDNA3.1 vector (Invitrogen). At 24 hours posttransfection, cells were harvested and the cell lysate was analyzed using a dual-luciferase reporter assay system (Promega). The ratio of firefly luciferase activity to *Renilla* luciferase activity in each sample served as a measure of normalized luciferase activity.

Small interfering RNA

siRNA of the mouse *c-Myc* gene was designed using BLOCK-iT RNAi Designer (Invitrogen). The siRNA oligonucleotide sequences were as follows: siRNA control sense, 5′-UAGUGUGAGCACUGUGAUUCCUUGG-3′ and antisense 5′-CCAAGGAUCACAGUGCUCACACUA-3′; *c-Myc* siRNA sense 5′-UAGUCGAGGUC-AUAGUUCCUGUUGG-3′ and antisense 5′-CCAACAGGAACUAUGACCUCGACUA-3′. The oligonucleotides were transfected into Colon 26 cells at a final concentration of 20 nmol/L using Lipofectamine 2000 (Invitrogen).

Chromatin immunoprecipitation assays

Tumor masses were excised and treated with 1% formaldehyde for 5 minutes at room temperature to cross-link the chromatin, and the reaction was stopped by adding glycine to a final concentration of 0.125 mol/L. Each cross-linked sample was sonicated on ice and then incubated with antibodies against c-MYC, CLOCK, rabbit-IgG, or goat-IgG (Santa Cruz Biotechnology). Chromatin/antibody complexes were extracted using a protein G agarose kit (Roche). DNA was isolated using the Wizard SV Genomic DNA Purification System (Promega) and subjected to PCR using the following primers for the c-MYC binding site (E-box) of the *TfR1* promoter region, forward 5′-GTGACTCCCTTGTCAG-3′ and reverse 5′-CCGTGACACTAGTAACC-3′. For PCR analysis, PCR products were amplified for 40 or 45 cycles. PCR products were run on an agarose (3%) gel, including 0.2 μg/mL ethidium bromide, and analyzed using the NIH image software.

Determination of L-OHP (Pt) concentration

Plasma samples were obtained by centrifugation at 3,000 rpm for 3 minutes and stored at −20°C until analysis. Tumor DNA was extracted using a Wizard Genomic DNA Purification kit (Promega). Measurements of the L-OHP (Pt) content in plasma and tumor DNA were made using ICP-MS at the Center of Advanced Instrumental Analysis, Kyushu University. ICP-MS is capable of detecting very small amounts of Pt. Plasma Pt concentration and its tumor DNA content were expressed as micrograms per milliliter and nanograms per nanogram of DNA, respectively.

Determination of the antitumor effect

Seven days after the inoculation of Colon 26 cells into mice, a single injection of Tf-NGPE L-OHP (L-OHP: 0, 7.5 mg/kg, i.v.) or vehicle (9% sucrose) was given to tumor-bearing mice at 9:00 a.m. or 9:00 p.m. This dosage of Tf-NGPE L-OHP was selected based on a preliminary study (Supplementary Data S3). In all mice, the tumor volumes were measured every 3 days throughout the duration of the experiment.

Statistical analysis

ANOVA was used for multiple comparisons, and Scheffe's test was used for comparison between two groups. A 5% level of probability was considered significant.

Results

Twenty-four-hour rhythm in the expression of TfR1 in Colon 26 tumor masses

Two subtypes of TfR have been identified: TfR1 and TfR2. In implanted Colon 26 cells, *TfR1* but not *TfR2* was detectable, although *TfR2* was expressed in mouse liver (Supplementary Data S1B). The protein and mRNA levels of TfR1 in implanted Colon 26 cells showed a significant 24-hour rhythm, with higher levels during the early dark phase ($P < 0.05$; Fig. 1A and B). The increase and decrease in mRNA levels of *TfR1* seemed to cause the rhythm of TfR1 protein in Colon 26 tumor masses.

Regulation of the 24-hour rhythm in the expression of *TfR1* gene by c-MYC

Among these, c-MYC is a potent activator of *TfR1* gene transcription in mice and humans, and the transactivation effect was elicited through binding to the CACGTG E-box located in the first intron region (18, 19). In addition, CLOCK/BMAL1 heterodimers also bind cooperatively to CACGTG E-box sequences and regulate the rhythmic expression of their target genes (2). Thus, to establish the relevance of the biological clock system on the expression of *TfR1*, CLOCKΔ19 (CLOCK protein lacking transcriptional activity) was overexpressed in Colon 26 cells. Clock mutant mice have

Published OnlineFirst July 14, 2010; DOI: 10.1158/0008-5472.CAN-10-0184

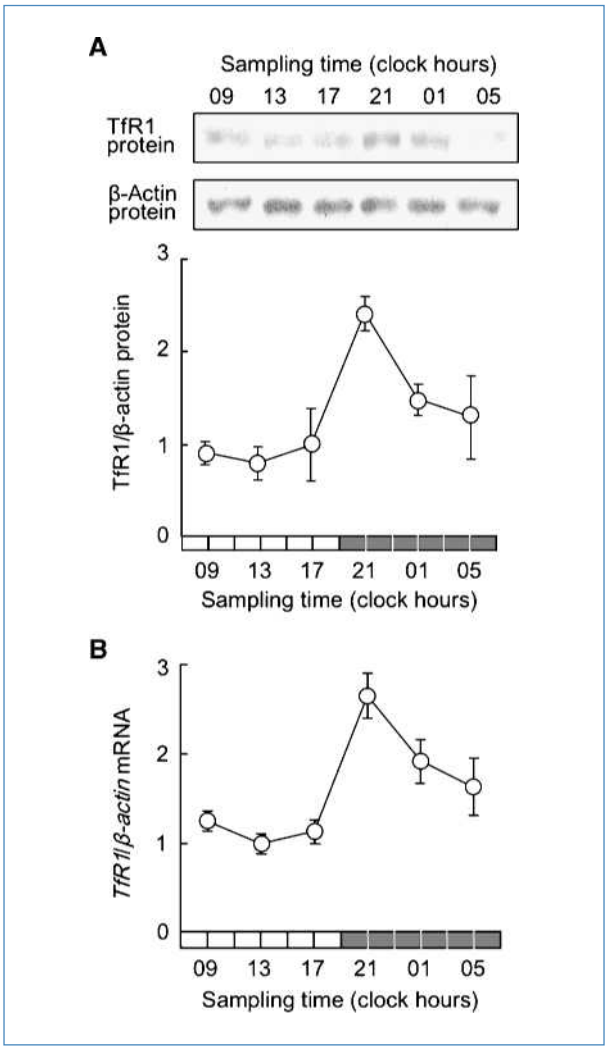

Figure 1. Twenty-four hour variation in the expression of TfR1 in Colon 26 tumor masses. A, temporal expression profile of TfR1 protein in tumor masses. The photographs show 24-h variation in TfR1 protein in implanted Colon 26 tumor cells. Cytoplasmic proteins were measured using each of the antibodies. Bottom, relative TfR1 protein levels. The data were normalized using β-actin as a control. Points, mean (n = 3, P < 0.01, ANOVA); bars, SEM. B, temporal expression profile of *TfR1* mRNA in tumor masses. The data are normalized using β-*actin* as a control. Points, mean (n = 6, P < 0.01, ANOVA); bars, SEM.

a point mutation in exon 19 of the *Clock* gene and exhibit low-amplitude rhythms in the expression of various genes (20). *TfR1* and *c-Myc* expression levels were low in CLOCKΔ19 overexpressing Colon 26 cells (Supplementary Data S4). Next, we tested whether these transcription factors participate in regulation of the rhythmic expression of *TfR1* gene in Colon 26 cells. Cotransfection of *TfR1*-Luc with c-MYC expression constructs resulted in an 8.1-fold increase in promoter activity, whereas CLOCK/BMAL1 had little effect on the transcriptional activity of the *TfR1* gene (Fig. 2B). The transactivation effect of c-MYC on *TfR1* reporters was dependent on the E-box element located from bp +290 to +295 because mutation of the CACGTG sequence to AAGCTT reduced transcriptional activation by c-MYC from 8.1- to 1.5-fold.

Several compounds and high concentration serum have been shown to induce and/or synchronize circadian gene expression in cultured cells (21). Thus, to elucidate the role of c-MYC in the circadian regulation of *TfR1* expression, the temporal expression profiles of *TfR1* mRNA in c-MYC–downregulated Colon 26 cells were investigated after 50% FBS treatment. Brief exposure of control scrambled siRNA-transfected cells to 50% FBS resulted in the oscillation of *TfR1* mRNA levels with a period length of ~24 hours (Fig. 3A). On the other hand, the protein levels of c-MYC were decreased and the mRNA levels of *TfR1* failed to show a significant 24-hour oscillation after the treatment of *c-Myc* siRNA–transfected cells with 50% FBS (Fig. 3B and C). These results suggested that c-MYC is required for generating the time-dependent variation in *TfR1* mRNA expression.

The transcription of *c-Myc* is regulated by components of the circadian clock, and its mRNA levels in mouse liver and bones have been shown to exhibit a significant 24-hour oscillation (22). The protein levels of c-MYC in Colon 26 cells implanted in mice also showed obvious 24-hour oscillations with higher levels around the early dark phase and lower levels during the early light phase, whereas there was no obvious 24-hour variation in the protein levels of CLOCK in the tumor

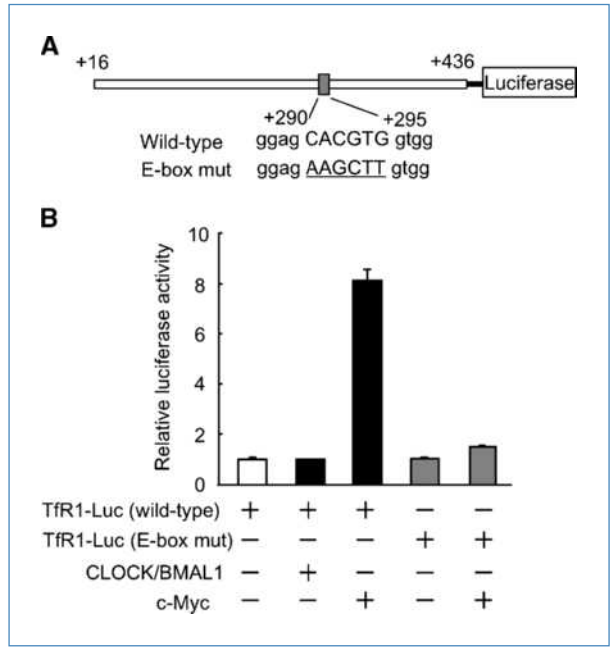

Figure 2. Influence of CLOCK/BMAL1 and c-MYC on transcription of the mouse *TfR1* gene. A, schematic representation of the mouse *TfR1* promoter. The numbers on both sites, the distance (bp) from the transcription start site (+1) included in the luciferase reporter construction. The numbers of nucleotide residues below the box, the positions of the E-box. The underlined nucleotide residues, the mutated sequence of the E-box. B, wild-type or E-box–mutated *TfR1* gene reporter plasmids (*TfR*1-Luc) were cotransfected with expression constructs encoding CLOCK/BMAL1 or c-MYC. Columns, mean (n = 3); bars, SEM.

Published OnlineFirst July 14, 2010; DOI: 10.1158/0008-5472.CAN-10-0184

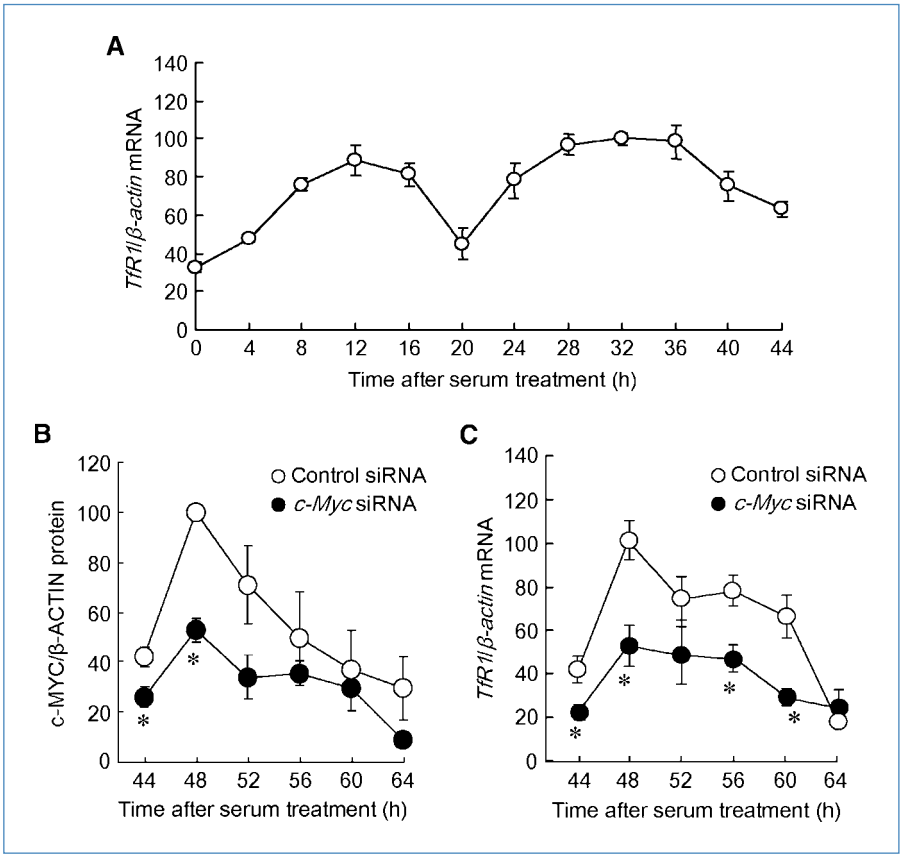

Figure 3. Influence of the downregulation of c-MYC on the rhythmic expression of *TfR1* mRNA in Colon 26 cells. A, temporal accumulation of *TfR1* mRNA in Colon 26 cells after 50% serum shock. The data are normalized using β-*actin* as a control. Points, mean ($n = 3$, $P < 0.01$, ANOVA); bars, SEM. Data are plotted relative to the 0-h value after 50% serum shock. B, temporal accumulation of c-MYC protein in control cells or c-Myc knockdown cells after 50% serum shock. Colon 26 cells were transfected with scrambled siRNA (control siRNA) or specific siRNA for c-Myc (c-Myc siRNA). Crude cell extracts were measured by Western blotting analysis. The data were normalized using β-actin as a control. Points, mean ($n = 3$, control cells; $P < 0.01$, ANOVA); bars, SEM. *; $P < 0.05$, when compared with the value for the control siRNA group at the corresponding times. C, temporal accumulation of *TfR1* mRNA in control cells or *c-Myc* knockdown cells. The mRNA levels of *TfR1* were determined at the indicated time points after serum treatment. Points, mean ($n = 3$, control cells; $P < 0.01$, ANOVA); bars, SEM. *, $P < 0.05$, when compared with the value for the control siRNA group at the corresponding times.

cells (Fig. 4A). The results of chromatin immunoprecipitation analysis revealed that endogenous c-MYC in Colon 26 cells bound to the E-box element in the intron region of *TfR1* gene (Fig. 4B). Of particular note, the binding amounts of c-MYC increasedat the time of day corresponding to the peak of *TfR1* mRNA expression (see Fig. 1B), suggesting that the time-dependent binding of c-MYC to the E-box in *TfR1* gene underlies its rhythmic expression. In addition, the mRNA levels of a prototypical c-MYC–regulated gene, telomerase reverse transcriptase (23), in Colon 26 cells implanted in mice also showed time-dependent variation (Supplementary Data S5).

Relationship between the rhythmic expression of TfR1 and time dependency of Pt incorporation into tumor DNA

Tf-NGPE L-OHP is a transferrin-conjugated liposome encapsulating L-OHP, a diaminocyclohexane Pt antitumor agent, which forms adducts with DNA. Tf-NGPE L-OHP binds to TfR, which is expressed on the plasma membrane and can internalize Pt into the cell.[3] Thus, to explore the function of internalization into the cell through transferrin in the rhythmic expression of TfR1, we investigated the temporal profile of *TfR1* gene expression and incorporation of Pt into tumor DNA in synchronized and desynchronized Colon 26 cells. A brief exposure of cultured Colon 26 cells to 50% FBS medium for 2 hours induced an oscillation in the expression of *TfR1* mRNA (Fig. 5A). The mRNA levels of *TfR1* peaked at 18 hours after treatment of the cells with 50% FBS. The oscillation of *TfR1* mRNA levels was also found on day 3 after serum treatment (see Fig. 3). The amount of Pt incorporated into the DNA of serum-shocked cells after treatment with Tf-NGPE L-OHP increased significantly at the time point corresponding to the peak in the level of TfR1 protein ($P < 0.05$; Fig. 5B). In contrast, in nontreated cells, neither the mRNA and protein levels of TfR1 nor Pt incorporation showed significant time-dependent variations (Fig. 5A and B), suggesting that the oscillation in the

[3] Our unpublished data.

Published OnlineFirst July 14, 2010; DOI: 10.1158/0008-5472.CAN-10-0184

expression of TfR1 underlies the time-dependent change in Pt incorporation into tumor DNA.

Influence of dosing time on the ability of Tf-NGPE L-OHP to inhibit tumor growth

The plasma Pt concentration decreased gradually after a single injection of 7.5 mg/kg Tf-NGPE L-OHP (i.v.) at both dosing times, but the Pt concentration in plasma at 3 hours after Tf-NGPE L-OHP injection was significantly higher in mice injected with the drug at 9:00 a.m. than at 9:00 p.m. (Fig. 6A, left). On the other hand, Pt incorporation into DNA in tumor cells at 3 and 6 hours after Tf-NGPE L-OHP injection was significantly higher in mice injected with the drug at 9:00 p.m. than at 9:00 a.m. (Fig. 6A, right). We also attempted to determine the Pt contents in tumor DNA at over 6 hours after Tf-NGPE L-OHP injection, but accurate assessment was difficult, probably due to L-OHP–induced apoptotic or necrotic tumor cell death.

A significant antitumor effect of Tf-NGPE L-OHP was observed when tumor-bearing mice were injected i.v. with a single dose of 7.5 mg/kg L-OHP (Supplementary Data S3). Thus, the dosage was set at 7.5 mg/kg to investigate whether the antitumor effect of Tf-NGPE L-OHP was altered depending on its dosing time. The growth of tumor cells was significantly suppressed by the administration of Tf-NGPE L-OHP (7.5 mg/kg, i.v.). The antitumor effects were more potent in mice injected with the drug at 9:00 p.m. than in those that received it at 9:00 a.m. (Fig. 6B). Fifteen days after injection of the drug, the tumor volume in mice injected with Tf-NGPE L-OHP at 9:00 p.m. was significantly smaller than that in mice injected at 9:00 a.m. ($P < 0.05$).

Discussion

TfR1 is a key cell surface molecule that regulates the uptake of iron-bound transferrin (8). It has been shown that correlation exists between the number of surface TfR1 and the rate of cell proliferation. TfR1 expression is higher in tumor cells than in normal cells. Thus, intracellular targeting using iron-saturated Tf as a ligand for TfR-mediated endocytosis has attracted attention. In this study, the protein abundance of TfR1 on Colon 26 tumor cells implanted in mice showed a clear 24-hour oscillation. The rhythmic phase of TfR1 protein

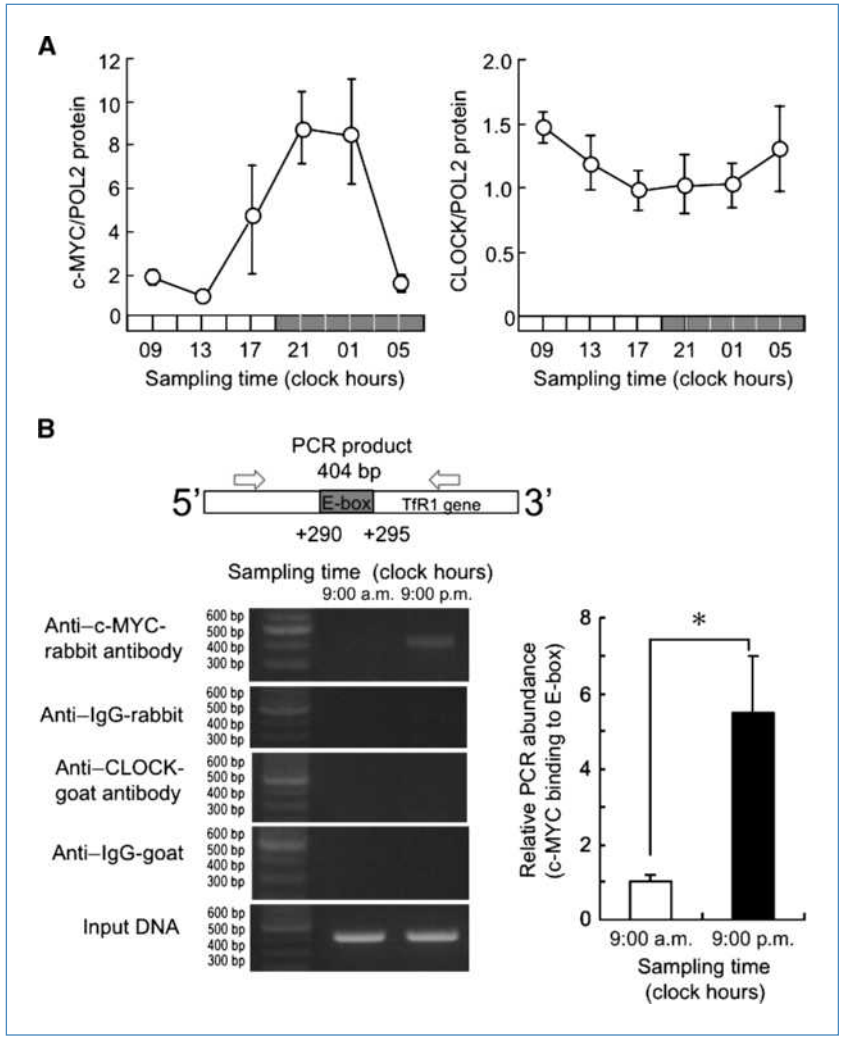

Figure 4. Time-dependent changes in the binding of endogenous c-MYC to the E-box element in the *TfR1* gene. A, temporal expression profiles of protein levels of c-MYC and CLOCK in implanted Colon 26 tumor masses. POL2 protein was used as an internal control whose expression was constant throughout the day. The data are normalized using POL2 as a control ($P < 0.01$, ANOVA). CLOCK protein did not show an obvious variation. Points, mean ($n = 3$); bars, SEM. B, left, temporal profiles of the binding of endogenous c-MYC to the *TfR1* gene in Colon 26 cells implanted in mice. Right, the quantification of temporal changes in the binding of c-MYC to the *TfR1* gene in Colon 26 cells implanted in mice. The mean value of each assay at 9:00 a.m. was set at 1. Columns, mean ($n = 3$); bars, SEM. *; $P < 0.05$ for the comparison between the two groups.

Published OnlineFirst July 14, 2010; DOI: 10.1158/0008-5472.CAN-10-0184

paralleled that of its mRNA levels. However, the mechanisms of transcriptional rhythm of TfR1 were unclear.

The molecular circadian clock operates at a cellular level and coordinates a wide variety of physiologic processes (24). CLOCK/BMAL1 heterodimers activate the transcription of *Per, Cry*, and *Dec* genes through CACGTG E-box enhancer elements (8). The results of luciferase reporter assays and chromatin immunoprecipitation experiments revealed that the CACGTG E-box located in the first intron of the mouse *TfR1* gene was unable to respond to CLOCK/BMAL1 heterodimers. In contrast, as reported previously (19), c-MYC could bind to the E-box of the mouse *TfR1* gene and activate its transcription. The amount of endogenous c-MYC protein binding to the mouse *TfR1* gene E-box fluctuated in a time-dependent manner. The binding of c-MYC to the E-box increased at the time corresponding to the peak of *TfR1* mRNA expression, suggesting that c-MYC acts as a regulator of circadian expression of the *TfR1* gene in Colon 26 tumor cells. This hypothesis was also supported by the present findings that the amplitude of the *TfR1* mRNA rhythm in serum-shocked Colon 26 cells was decreased by the down-regulation of c-MYC. On the other hand, CLOCK protein did not bind to the *TfR1* gene E-box. This may account for the unresponsiveness of the *TfR1* gene to CLOCK/BMAL1 heterodimers. The sequence surrounding the E-box and its location had a marked influence on the transcriptional activity of CLOCK/BMAL1 (6). In fact, a CT-rich *cis*-acting element of the mouse vasopressin gene confers robust CLOCK/BMAL1 responsiveness on an adjacent E-box (25). The absence of such a CT-rich *cis*-acting element around the E-box may result in the inability of CLOCK/BMAL1 to transactivate the mouse *TfR1* gene.

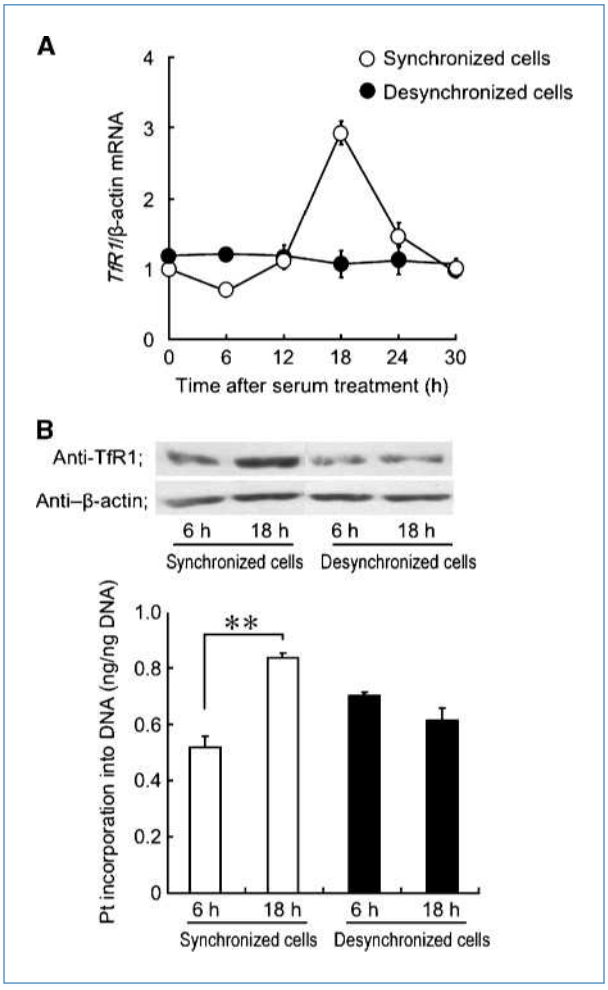

Figure 5. Influence of rhythmic changes in the expression of TfR1 on intratumoral delivery of L-OHP by Tf-NGPE liposomes. A, the temporal expression profile of *TfR1* mRNA in synchronized (○) or unsynchronized (•) Colon 26 cells. Cultured Colon 26 cells were synchronized by exposure to 50% FBS for 2 h. Points, mean (n = 3, synchronized cells; $P < 0.05$, ANOVA); bars, SEM. B, the photographs show temporal expression of TfR1 protein in synchronized or unsynchronized Colon 26 cells. Bottom, that temporal profile of Pt incorporation into DNA in synchronized or unsynchronized Colon 26 cells. Cells were exposed to Tf-NGPE L-OHP (L-OHP: 0.4 mg/mL) for 3 h at 6 or 18 h after the serum treatment, and then the amounts of Pt incorporated into tumor DNA were measured. Columns, mean (n = 3); bars, SEM. *, $P < 0.05$ for the comparison between the two time points.

Because the rhythmic phase of c-MYC protein abundance in Colon 26 cells correlated with the time dependency of its binding to the *TfR1* gene E-box, the oscillation in c-MYC protein levels may cause the 24-hour rhythm in the expression of downstream genes by rhythmic binding to their DNA response elements. In fact, *mTERT* mRNA in implanted Colon 26 tumor also showed time-dependent variation. In addition, *c-Myc* is regulated by clock genes, as indicated by previous results (26). *TfR1* and *c-Myc* expression levels were low in CLOCKΔ19-overexpressing Colon 26 cells. Although the E-box of the *TfR1* gene did not respond to CLOCK/BMAL1, the molecular components of the circadian clock may indirectly regulate the expression of the *TfR1* gene in Colon 26 cells.

It was reported previously that L-OHP could accumulate in tumor masses following delivery using Tf-PEG liposomes (16). TfR-targeting liposomes also bind to TfR on tumor cell surfaces and are internalized into the cells by receptor-mediated endocytosis. In this study, to evaluate the function of the 24-hour oscillation in TfR1, Tf-NGPE liposomes were used as a targeting carrier for intratumoral delivery of L-OHP. This TfR-targeting liposomal DDS exhibited similar pharmacokinetic properties to Tf-PEG liposomes, and i.v. administration of L-OHP encapsulated within Tf-NGPE liposomes lead to the accumulation of a high concentration of L-OHP in tumors as much as Tf-PEG liposomes.[4] The amount of Pt in tumor DNA after Tf-NGPE L-OHP injection increased at the times of day when TfR1 was abundant on the tumor surface in this study. This notion was also supported by *in vitro* findings that the time dependency of Tf-NGPE liposome–delivered L-OHP into tumor cells disappeared in the absence of the oscillation in TfR1 expression. These findings suggest that the oscillation in the expression of TfR1 underlies the dosing time–dependent changes in the internalization into

[4] Our unpublished data.

Published OnlineFirst July 14, 2010; DOI: 10.1158/0008-5472.CAN-10-0184

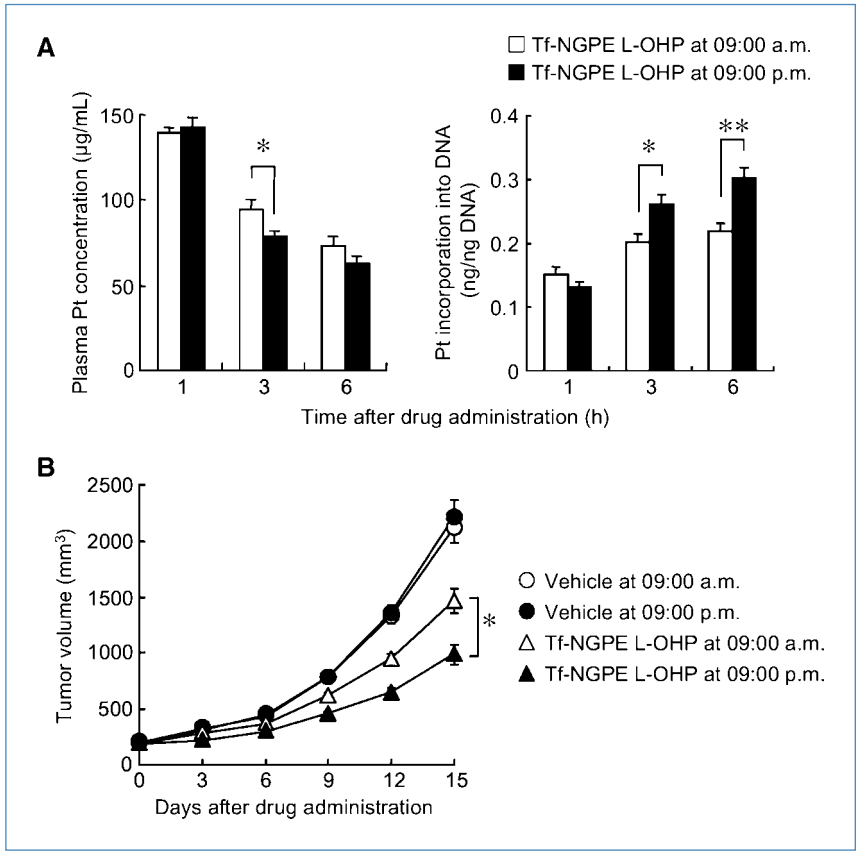

Figure 6. Influence of dosing time on the ability of Tf-PEG L-OHP to inhibit tumor growth in mice. Colon 26 tumor–bearing mice were injected i.v. with a single dose of Tf-NGPE L-OHP (L-OHP: 7.5 mg/kg) or vehicle (9% sucrose) at 9:00 a.m. or 9:00 p.m. A, dosing time–dependent differences in the intratumoral delivery of L-OHP by Tf-NGPE liposomes were examined. Plasma Pt concentration (left) and Pt incorporation into tumor DNA (right) were measured at the indicated times after an injection of Tf-NGPE L-OHP. Columns, mean (n = 5); bars, SEM; **, $P < 0.01$; *, $P < 0.05$ for comparison between the two groups. B, dosing time–dependent difference in the antitumor effect of Tf-NGPE L-OHP. Points, mean (n = 8–10); bars, SEM; *, $P < 0.05$ for comparison between the two dosing times.

the cells by receptor-mediated endocytosis. In addition, after a single injection of Tf-NGPE L-OHP, the antitumor effect of the drug varied according to its dosing time. The dosing time dependency of the antitumor effect seemed to be caused by time-dependent changes in the intratumoral delivery of L-OHP by TfR-targeting liposomes.

In the present study, it was shown that the 24-hour rhythm of TfR1 expression in colon cancer cells was controlled by c-MYC, and the cyclical accumulation of TfR1 caused dosing time–dependent changes in the intratumoral delivery of L-OHP by receptor-mediated endocytosis. Identification of the circadian properties of molecules that are targeted by ligand-directed DDS may aid the choice of the most appropriate time of day for their administration.

Disclosure of Potential Conflicts of Interest

The authors disclose no conflicts.

Grant Support

Grants-in-Aid for Scientific Research on Priority Areas "Cancer" (S.O. 20014016) from the Ministry of Education, Culture, Sport, Science and Technology of Japan, for Scientific Research (B; S.O. 21390047), for Challenging Exploratory Research (S.O. 21659041), and for the Encouragement of Young Scientists (N.M. 20790137) from the Japan Society for the Promotion of Science.

The costs of publication of this article were defrayed in part by the payment of page charges. This article must therefore be hereby marked *advertisement* in accordance with 18 U.S.C. Section 1734 solely to indicate this fact.

Received 01/18/2010; revised 06/07/2010; accepted 06/07/2010; published OnlineFirst 07/14/2010.

References

1. Stephan FK, Zucker I. Circadian rhythms in drinking behavior and locomotor activity of rats are eliminated by hypothalamic lesions. Proc Natl Acad Sci U S A 1972;69:1583–6.
2. Alvarez JD, Sehgal A. Circadian rhythms: finer clock control. Nature 2002;419:798–9.
3. Gekakis N, Staknis D, Nguyen HB, et al. Role of the CLOCK protein in the mammalian circadian mechanism. Science 1998;280:1564–9.
4. Kume K, Zylka MJ, Sriram S, et al. mCRY1 and mCRY2 are essential components of the negative limb of the circadian clock feedback loop. Cell 1999;98:193–205.
5. Preitner N, Damiola F, Lopez-Molina L, et al. The orphan nuclear receptor REV-ERBα controls circadian transcription within the positive limb of the mammalian circadian oscillator. Cell 2002;110:251–60.
6. Sato TK, Yamada RG, Ukai H, et al. Feedback repression is required for mammalian circadian clock function. Nat Genet 2006;38:312–9.

Published OnlineFirst July 14, 2010; DOI: 10.1158/0008-5472.CAN-10-0184

7. Koyanagi S, Kuramoto Y, Nakagawa H, et al. A molecular mechanism regulating circadian expression of vascular endothelial growth factor in tumor cells. Cancer Res 2003;63:7277–83.
8. Daniels TR, Delgado T, Helguera G, Penichet ML. The transferrin receptor part II: targeted delivery of therapeutic agents into cancer cells. Clin Immunol 2006;121:159–76.
9. Sorokin LM, Morgan EH, Yeoh GC. Transformation-induced changes in transferrin and iron metabolism in myogenic cells. Cancer Res 1989;49:1941–7.
10. Niitsu Y, Kohgo Y, Nishisato T, et al. Transferrin receptors in human cancerous tissues. Tohoku J Exp Med 1987;153:239–43.
11. Calzolari A, Oliviero I, Deaglio S, et al. Transferrin receptor 2 is frequently expressed in human cancer cell lines. Blood Cells Mol Dis 2007;39:82–91.
12. Kawabata H, Nakamaki T, Ikonomi P, Smith RD, Germain RS, Koeffler HP. Expression of transferrin receptor 2 in normal and neoplastic hematopoietic cells. Blood 2001;98:2714–9.
13. Röhrs S, Kutzner N, Vlad A, Grunwald T, Ziegler S, Müller O. Chronological expression of Wnt target genes Ccnd1, Myc, Cdkn1a, TfRc, Plf1 and Ramp3. Cell Biol Int 2009;33:501–8.
14. Papahadjopoulos D, Allen TM, Gabizon A, et al. Sterically stabilized liposomes: improvements in pharmacokinetics and antitumor therapeutic efficacy. Proc Natl Acad Sci U S A 1991;88:11460–4.
15. Ishida O, Maruyama K, Tanahashi H, et al. Liposomes bearing polyethyleneglycol-coupled transferrin with intracellular targeting property to the solid tumors *in vivo*. Pharm Res 2001;18:1042–8.
16. Suzuki R, Takizawa T, Kuwata Y, et al. Effective anti-tumor activity of oxaliplatin encapsulated in transferrin-PEG-liposome. Int J Pharm 2008;346:143–50.
17. Ohdo S, Koyanagi S, Suyama H, Higuchi S, Aramaki H. Changing the dosing schedule minimizes the disruptive effects of interferon on clock function. Nat Med 2001;3:356–60.
18. Holloway K, Sade H, Romero IA, Male D. Action of transcription factors in the control of transferrin receptor expression in human brain endothelium. J Mol Biol 2007;365:1271–84.
19. O'Donnell KA, Yu D, Zeller KI, et al. Activation of transferrin receptor 1 by c-Myc enhances cellular proliferation and tumorigenesis. Mol. Cell Biol 2006;26:2373–86.
20. Oishi K, Miyazaki K, Kadota K, et al. Genome-wide expression analysis of mouse liver reveals CLOCK-regulated circadian output genes. J Biol Chem 2003;278:41519–27.
21. Takiguchi T, Tomita M, Matsunaga N, Nakagawa H, Koyanagi S, Ohdo S. Molecular basis for rhythmic expression of CYP3A4 in serum-shocked HepG2 cells. Pharmacogenet Genomics 2007;17:1047–56.
22. Wittekindt NE, Hörtnagel K, Geltinger C, Polack A. Activation of c-*myc* promoter P1 by immunoglobulin κ gene enhancers in Burkitt lymphoma: functional characterization of the intron enhancer motifs κB, E box 1 and E box 2, and of the 3′ enhancer motif PU. Nucleic Acids Res 2000;28:800–8.
23. Reymann S, Borlak J. Transcription profiling of lung adenocarcinomas of c-*myc*-transgenic mice: identification of the c-*myc* regulatory gene network. BMC Syst Biol 2008;2:46.
24. Weaver ReppertSM. Coordination of circadian timing in mammals. Nature 2002;418:935–41.
25. Muñoz E, Brewer M, Baler R. Modulation of BMAL/CLOCK/E-Box complex activity by a CT-rich *cis*-acting element. Mol Cell Endocrinol 2006;252:74–81.
26. Fu L, Pelicano H, Liu J, Huang P, Lee C. The circadian gene Period2 plays an important role in tumor suppression and DNA damage response *in vivo*. Cell 2002;111:41–50.

AACR American Association for Cancer Research

Cancer Research

The Journal of Cancer Research (1916–1930) | The American Journal of Cancer (1931–1940)

Circadian Rhythm of Transferrin Receptor 1 Gene Expression Controlled by c-Myc in Colon Cancer–Bearing Mice

Fumiyasu Okazaki, Naoya Matsunaga, Hiroyuki Okazaki, et al.

Cancer Res 2010;70:6238-6246. Published OnlineFirst July 14, 2010.